

Numerical Study of Microbeam with Geometric Discontinuity Under Electrostatic Load using Strain Gradient Theory

Hadi Hamidizadeh, Mahmoud Mousavi Mashhadi*,
Younes Mohammadi

Department of Mechanical Engineering, Faculty of Industrial and
Mechanical Engineering, Qazvin Branch, Islamic Azad University,
Qazvin, Iran.

E-mail: h.hamidizadeh@yahoo.com, m.mosavi@qiau.ac.ir*,
u.mohammadi@gmail.com

*Corresponding author

Received: 7 August 2019, Revised: 10 January 2020, Accepted: 2 February 2020

Abstract: In this work, the pull in analysis of microbeam with geometric discontinuity for two different boundary conditions has been investigated. Boundary conditions are considered as Clamped-Free (CF) and Clamped-Clamped (CC). The governing equations are transformed into non-dimensional form and then solved using Differential Quadrature method (DQ). The conductive polymer length scale parameter was also obtained. The effects of different parameters and pull in voltage on microbeam are studied. Most of the microbeams analyzes were made of Gold, Nickel or Silicon, but we used variety of conductive polymers in this paper. The results show that conductive polymer microbeams can be a suitable substitute for expensive metals. The results can be used to design and improve the performance of Micro-Electromechanical System (MEMS) devices.

Keywords: Conductive Polymer, Differential Quadrature Method, Electrostatic, Strain Gradient

Reference: Hadi Hamidizadeh, Mahmoud Mousavi Mashhadi and Younes Mohammadi, "Numerical Study of Microbeam with Geometric Discontinuity Under Electrostatic Load using Strain Gradient Theory", Int J of Advanced Design and Manufacturing Technology, Vol. 13/No. 1, 2020, pp. 59–68.

Biographical notes: Hadi Hamidizadeh is a PhD candidate in Mechanical Engineering in IAU, Qazvin Branch. His current research interest includes MEMS, smart materials and composites. Mahmoud Mousavi Mashhadi is Professor of Mechanical Engineering at the IAU, Qazvin Branch. He received his PhD in Mechanical Engineering from Arkansas University of America. His current research focuses on MEMS and Manufacturing. Younes Mohammadi is Assistant Professor of Mechanical Engineering at the IAU, Qazvin Branch. He received his PhD in Mechanical Engineering from KNT University of Iran. His current research focuses on MEMS, vibration, smart materials and composites.

1 INTRODUCTION

The need to minimize the complex of sensor, processor, operator assemblies and integrate them into a single chip has led to the invention of the finest human fabrications called microelectromechanical systems (MEMS). So accurate modeling and providing suitable methods for solving equations governing their mechanical behavior is of great importance. Microbeam with geometric discontinuity are widely used in MEMS industries.

A micropositioning system is a motioning system composed of different mechanical and electrical components capable of producing displacements in micro scale. Such equipments are used in systems to produce displacements in the order of micro meter. Some of the important applications of this equipment are in semiconductors, optic and laser industries, sweeping microscopes, precise machining, genetic manipulations and inter-cellular activities [1]. The main function of these systems is based on the deformation of a beam in micro size. Therefore, study of the behavior and control of microbeams will be of great importance in science and engineering. Micro/nano actuators are made of two electrodes in a micro/nano electromechanical system, one of them is movable and flexible and the other is fixed, the moving electrode is suspended above the substrate electrode. The applied voltage between the two electrodes causes the displacement of the moving electrode and its displacement towards the substrate (or fixed) electrode. When the voltage between two electrodes is increased from a certain value, the system becomes unstable and the contact between the two electrodes is created. This phenomenon is called the Pull-in instability and the voltage corresponding to that is the Pull-in voltage [2]. Over the past several decades, there has been a lot of research on micro and nano-sized structures, which we will cover a few. Sadeghi et al. [3] Investigated the size-dependent behavior of a microbeam under the influence of a nonlinear electrostatic pressure. They found that there is significant difference between the Pull-in voltages obtained from classical theory and modified couple stress theory, where previous researchers who used classical theory used a large amount of tensile residual stress of their modeling. However, the results of this research show that the use of modified couple stress theory significantly reduces the difference between theoretical and experimental results. Zhu et al. [4] reviewed the behavior of the Pull-in stepped microbeam using the modified couple stress theory. They found that the natural frequency as well as the Pull-in voltage increased with increasing width ratios uniformly, but with increasing length ratio, first decreases and then increases. Habibnejad korayem et al. [5] Analyzed the piezoelectric and geometric discontinuities of an atomic force microscopy using the modified couple stress

theory and they used DQ method to solve them. The results showed that the length scale parameter does not only affect the frequency and amplitude but also improves the accuracy of the results compared to the classical theory. In addition, the effects of geometric parameters on the piezoelectric frequency are also investigated. Rahaeifard and Ahmadian [6], investigated instability of microbeam under the electrostatic load using the strain gradient theory and Hamilton principle and compared their results with the results of the classical theory as well as the modified couple stress theory. The results of strain gradient theory and modified couple stress theory were well convergent. Rahaeifard et al. [7], studied the deflection and pull-in voltage of microbeam, using the modified couple stress theory. They compared their research results with experimental results and classical theory, and used a finite difference method to solve them and found that there was a difference between experimental observations and classical theory, but they achieved better convergence with the results of the theory. Zhu and Liu [8] analyzed sensitivity of pull-in voltage for a stepped cantilever-type Radio Frequency (RF) MEMS switch, based on modified couple stress theory, they discovered the pull-in voltage sensitivity of design parameters. The optimal value of the dimensionless length ratio only depends on the dimensionless width ratio. Static and dynamic modeling of pull-in instability of a nanobeam was performed by Sadeghi et al. [9] using the strain gradient theory and reduced order method. The results showed that when the nano-actuator thickness is comparable with the material length scales, the size effect can significantly affect the tensile behavior of the system. It was also found that pull-in static voltage was greater than the dynamic voltage due to the inertia force. Wang and Duan [10] provided a discrete singular convolution method for static analysis, buckling, and free vibration of beam. They considered the Euler-Bernoulli model and proved the application of the above method to a beam with geometric discontinuity. Fathalilou and Rezaee [11] presented two methods for solving the electrostatic micro sensors vibrational equation. In the first method, first the two sides of the governing equation were multiplied by the reversal of the electrostatic force, then the Galerkin method was applied. Although in the second method, the Galerkin method was directly applied to the governing differential equation. They concluded that the first method was not able to detect pull-in point in some cases.

Up until about forty years ago, all carbon-based polymers were insulated, and the idea of plastic conductivity was meaningless and in the electrical industry, plastics were widely used as insulators. This attitude was quickly changed by the discovery of conductive polymers. In 1958, Shirakawa and colleagues produced a black polyacetylene powder,

which determined that the product obtained could have semi-conductivity to conductivity, depending on its conditions. Among the most common conductive polymers, polythiophene, polyaniline and polypyrrole are mentioned [12]. The electrical, electrochemical, optical conductivity polymers have converted them as a material for use in antistatic coatings, anti-corrosion coatings, coatings for absorbing microwave waves, biosensors. The conductivity properties of the polymers are adjustable to the desired degree, so that it can be in the form of conductors or semiconductors. These polymers are structurally in their main chain of dual band as one, so that their conductivity properties increase during the process of doping. The term doping is taken from the dictionary of semiconductor bodies because the receiver and electron donor material can increase the conductivity of conjugated polymers. The term doping is synonymous with oxidation or reduction. Valentova and Stejskal [13] have obtained the mechanical properties of polyaniline conductive polymer, such as the Young modulus and the Bulk modulus. Lang and et al. [14] obtained the mechanical properties of conductive polymer (PEDOT) by two methods of tensile testing, and also using an Atomic force microscopy and compared with each other. Cho et al. [15] analyzed the synthesis methods, electrochemical, and the size effect of polyaniline coated with polymetal. Zhang and Chu [16] studied the electrostatic actuated of conductive polymer microbridges. They used three different types of conductive polymers and they found the stability and conductivity of these materials. Moreover, the results of the Pull-in voltage, deflection and resonance phenomenon showed that mechanical properties have improved with the effect of residual stress in MEMS polymer structures. Kumar et al. [17] Investigated the synthesis methods, properties and applications of conductive polymers in various fields.

In this paper, strain gradient theory is employed to investigate the size dependent pull-in of the microbeam. The microbeam has a geometric discontinuity and is considered as a step. In addition, by applying the Galerkin method and numerical differential quadrature method, static analysis and the effect of different parameters are examined. The length scale parameter of the Polyaniline that is one of the conductive polymers, was obtained which recently researchers use them in the MEMS industries.

2 THEORETICAL MODEL

2.1. Fundamentals of Strain Gradient Theory

In this section, a review of the structural relations of the strain gradient theory will be presented according to the below section. In this theory, there are three independent

of length scale parameters in the constitutive equations in addition to the two classical constant of material, which the constitutive equations are dependent to the size of material. The strain energy (U) in a homogeneous elastic material in the domain of Ω can be obtained as follows [18-19]:

$$U = \frac{1}{2} \int_{\Omega} (\sigma_{ij} \varepsilon_{ij} + P_i \gamma_i + \tau_{ijk}^{(1)} \eta_{ijk}^{(1)} + m_{ij}^s \chi_{ij}^s) dv \quad (1)$$

The strain relations given above are obtained using the following relationships:

$$\varepsilon_{ij} = \frac{1}{2} (\partial_i u_j + \partial_j u_i) \quad (2)$$

$$\gamma_i = \partial_i \varepsilon_{mm} \quad (3)$$

$$\eta_{ijk}^{(1)} = \frac{1}{3} (\partial_i \varepsilon_{jk} + \partial_j \varepsilon_{ki} + \partial_k \varepsilon_{ij}) - \frac{1}{15} \delta_{ji} (\sigma_k \varepsilon_{mm} + 2\partial_m \varepsilon_{mk}) - \frac{1}{15} [\delta_{jk} (\partial_i \varepsilon_{mm} + 2\partial_m \varepsilon_{mi}) + \delta_{ki} (\partial_j \varepsilon_{mm} + 2\partial_m \varepsilon_{mj})] \quad (4)$$

$$\chi_{ij}^s = \frac{1}{2} (C_{ipq} \partial_p \varepsilon_{qj} + C_{ipq} \partial_p \varepsilon_{qi}) \quad (5)$$

Where, ε_{ij} , $\eta_{ijk}^{(1)}$, γ_i , and χ_{ij}^s are strain tensor, dilatation gradient vector, deviatoric stretch and symmetric rotation gradient tensor, respectively. u_i is displacement vector and δ^{ij} is Kronocker Delta. In addition, the stresses corresponding to the parameters $\eta_{ijk}^{(1)}$, γ_i , ε_{ij} and χ_{ij}^s , respectively, can be defined by σ_{ij} , P_i , $\tau_{ijk}^{(1)}$, m_{ij}^s . It is shown that σ_{ij} , the classic stress tensor, P_i , $\tau_{ijk}^{(1)}$, m_{ij}^s describe higher order tensors that are obtained using the following relationships:

$$\sigma_{ij} = k \delta_{ij} \varepsilon_{mm} + 2G \varepsilon'_{ij} \quad (6)$$

$$P_i = 2Gl_0^2 \gamma_i \quad (7)$$

$$\tau_{ijk}^{(1)} = 2Gl_1^2 \eta_{ijk}^{(1)} \quad (8)$$

$$m_{ij}^s = 2Gl_2^2 \chi_{ij}^s \quad (9)$$

$$\varepsilon'_{ij} = \varepsilon_{ij} - \frac{1}{3} \varepsilon_{mm} \delta_{ij} \quad (10)$$

Where, l_0 , l_1 and l_2 are additional material length scale parameters which appear in the constitutive of higher order stresses. Moreover, K and G are the bulk and shear modulus of material, using the E Young modulus and ν Poisson's ratio which are obtained

$$K = \frac{\nu E}{(1 + \nu)(1 - 2\nu)} \quad \text{and} \quad G = \frac{E}{2(1 + \nu)}$$

Respectively.

2.2. Microbeam Model

Figures 1 and 2 show the typical electrostatically actuated stepped microbeams with CF and CC boundary condition, respectively, the microbeam consists of a fixed electrode and a movable electrode with length of L and thickness of h which are separated by a dielectric spacer with an initial gap g_0 .

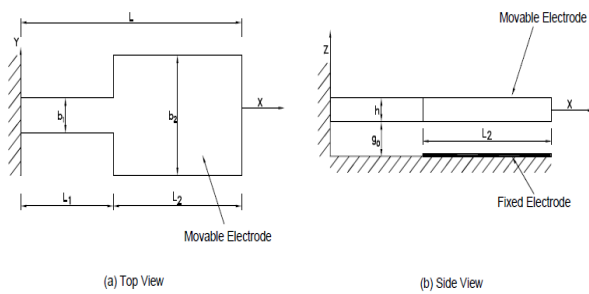


Fig. 1 Top and side view of stepped CF microbeam.

The movable electrode can be viewed as a beam of length L , width b_1 and thickness h with a rectangular pad of length L_2 , width b_2 and thickness h at its tip for micro cantilevers. The fixed electrode is the same size as the rectangular pad and is positioned under the pad.

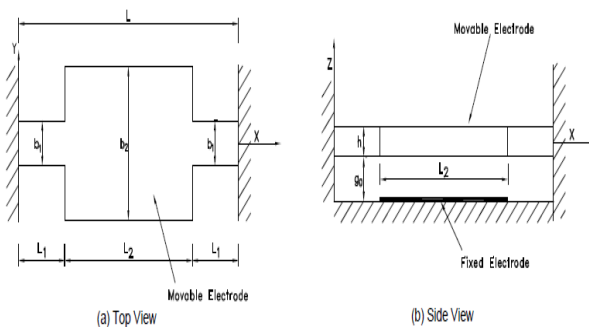


Fig. 2 Top and side view of stepped CC microbeam.

The origin of the Cartesian coordinate system is located at the middle of the left end of the stepped microbeams where X , Y and Z are the coordinates along the length, width and thickness, respectively. Note that the consideration of stretching and that of axial tractions along the beam is beyond the scope of this work and these effects are neglected in this research.

By substituting the displacement components in “Eqs. (2 to 10)” and then by replacing resultant of them in Eq. (1) the bending strain energy, U_m can be obtained by the following form:

$$U_m = \frac{1}{2} \int_0^{L_1} \left\{ \lambda [EI_1 + 2GA_1 l_0^2 + \frac{8}{15} GA_1 l_1^2 + GA_1 l_2^2] \left(\frac{\partial^2 w_1}{\partial x^2} \right)^2 + I_1 [2GI_0^2 + \frac{4}{5} GI_1^2] \left(\frac{\partial^3 w_1}{\partial x^3} \right)^2 \right\} dx + \frac{1}{2} \int_{L_1}^{L_1+L_2} \left\{ \lambda [EI_2 + 2GA_2 l_0^2 + \frac{8}{15} GA_2 l_1^2 + GA_2 l_2^2] \left(\frac{\partial^2 w_2}{\partial x^2} \right)^2 + I_2 [2GI_0^2 + \frac{4}{5} GI_1^2] \left(\frac{\partial^3 w_2}{\partial x^3} \right)^2 \right\} dx \quad (11)$$

The following equation is also added to the strain energy relation for the CC beam:

$$\frac{1}{2} \int_{L_1+L_2}^{L_1+L_2+L_1} \left\{ \lambda [EI_1 + 2GA_1 l_0^2 + \frac{8}{15} GA_1 l_1^2 + GA_1 l_2^2] \left(\frac{\partial^2 w_3}{\partial x^2} \right)^2 + I_1 [2GI_0^2 + \frac{4}{5} GI_1^2] \left(\frac{\partial^3 w_3}{\partial x^3} \right)^2 \right\} dx \quad (12)$$

Where, $I_1 = \frac{1}{12} b_1 h^3$ and $I_2 = \frac{1}{12} b_2 h^3$ are the cross sectional area moment of inertia and w_i is the beam deflection of microbeam. For CF beam, $i = 1, 2$, and For CC beam, $i = 1, 2, 3$. By applying the voltage V , the movable electrode bends to the fixed electrode under electrostatic force on the beam from $X = L_1$ to $X = L_1 + L_2$. The electrical potential energy U_e is the total electrostatic energy between the movable and fixed electrodes of the beam as follows:

$$U_e = -\frac{1}{2} V^2 \int_{L_1}^{L_1+L_2} dC \quad (13)$$

Where, V is the applied voltage and DC is the parallel plate capacitance per unit length between the fixed and movable electrodes:

$$dC = \frac{\epsilon_0 \epsilon_r b_2}{g_0 - w_2} \quad (14)$$

In the above equation, $\epsilon_0 = 8.854 \times 10^{-12} \text{ C}^2 \text{ N}^{-1} \text{ m}^{-2}$ is the permittivity of the free space and $\epsilon_r = 1$ is the dielectric coefficient of the dielectric medium between

the movable and fixed electrodes, and finally, we use (13) and (14), [20].

$$U_e = -\frac{V^2}{2} \int_{L_1}^{L_1+L_2} \left[\frac{\epsilon_0 b_2}{(g_0 - w_2)^2} (1 + 0.65 \frac{g_0 - w_2}{b_2}) \right] dx \quad (15)$$

The second term on the right hand side of “Eq. (15)” is the fringing field due to the finite width of the beam. The kinetic energy of the beam is also expressed as follows:

$$T = \frac{1}{2} \rho A_1 \int_0^{L_1} (\frac{\partial w_1}{\partial t})^2 dx + \frac{1}{2} \rho A_2 \int_{L_1}^{L_1+L_2} (\frac{\partial w_2}{\partial t})^2 dx \quad (16)$$

The following statement is also added for CC beam to the kinetic energy relation:

$$\frac{1}{2} \rho A_1 \int_{L_1+L_2}^{L_1+L_2+L_1} (\frac{\partial w_3}{\partial t})^2 dx \quad (17)$$

Where, ρ is mass density of the beam material, $A_1 = b_1 h$ and $A_2 = b_2 h$ are the cross sectional area of the beam. Now, the governing equations can be obtained using the [21] Hamilton’s principle

$$\delta \int_{t_1}^{t_2} (T - (U_m + U_e)) dt = 0.$$

$$\left\{ \begin{array}{l} \beta(1+B_1\mu_s) \frac{\partial^4 \bar{w}_1}{\partial x^4} \\ -\beta B_3 (\frac{\mu_s}{30B_2}) \frac{\partial^6 \bar{w}_1}{\partial x^6} = 0, \quad 0 \leq x \leq x_l \quad CF, CC \\ (1+B_1\mu_s) \frac{\partial^4 \bar{w}_2}{\partial x^4} - B_3 (\frac{\mu_s}{30B_2}) \frac{\partial^6 \bar{w}_2}{\partial x^6} \\ -\frac{\lambda^2}{4(1-\bar{w}_2(x))^2} (1+0.65\gamma(1-\bar{w}_2(x))) = 0, \quad x_l \leq x \leq x_u \quad CF, CC \\ \beta(1+B_1\mu_s) \frac{\partial^4 \bar{w}_3}{\partial x^4} \\ -\beta B_3 (\frac{\mu_s}{30B_2}) \frac{\partial^6 \bar{w}_3}{\partial x^6} = 0. \quad x_u \leq x \leq 1 \quad CC \end{array} \right. \quad (18)$$

In order to simplify the parametric calculations, the governing equations and boundary conditions can be converted to dimensionless state. Creating dimensionless parameters creates new concepts and better describes physical phenomena. The dimensionless variables $\bar{w} = \frac{w_i}{g_0}$, $\bar{x} = \frac{x}{L}$, and $\tau = \frac{t}{t_0}$ are used to simulate the governing equations and boundary conditions (Static state). The governing equation of the

system can be derived as the Eq. (18), with the following boundary conditions:

$$\left\{ \begin{array}{l} \bar{w}_1(0) = \frac{\partial \bar{w}_1(0)}{\partial x} = 0, \quad CF, CC \\ \bar{w}_1(x_l) = \bar{w}_2(x_l), \frac{\partial \bar{w}_1(x_l)}{\partial x} = \frac{\partial \bar{w}_2(0)}{\partial x}, \quad CF, CC \\ \beta B_3 (\frac{\mu_s}{30B_2}) \frac{\partial^3 \bar{w}_1(x_l)}{\partial x^3} = B_3 (\frac{\mu_s}{30B_2}) \frac{\partial^3 \bar{w}_2(x_l)}{\partial x^3}, \quad CF, CC \\ B_3 (\frac{\mu_s}{30B_2}) \frac{\partial^3 \bar{w}_2(1)}{\partial x^3} = 0, B_3 (\frac{\mu_s}{30B_2}) \frac{\partial^3 \bar{w}_2(0)}{\partial x^3} = 0, \quad CF \\ \frac{\partial^2 \bar{w}_2(1)}{\partial x^2} = \frac{\partial^3 \bar{w}_2(1)}{\partial x^3} = 0, \quad CF \\ \bar{w}_2(x_u) = \bar{w}_3(x_u), \frac{\partial \bar{w}_2(x_u)}{\partial x} = \frac{\partial \bar{w}_3(x_u)}{\partial x}, \quad CC \\ -(1+B_1\mu_s) \frac{\partial^3 \bar{w}_2(1)}{\partial x^3} + B_3 (\frac{\mu_s}{30B_2}) \frac{\partial^5 \bar{w}_2(1)}{\partial x^5} = 0, \quad CC \\ (1+B_1\mu_s) \frac{\partial^2 \bar{w}_2(1)}{\partial x^2} + B_3 (\frac{\mu_s}{30B_2}) \frac{\partial^4 \bar{w}_2(1)}{\partial x^4} = 0, \quad CC \\ \bar{w}_3(1) = \frac{\partial \bar{w}_3(1)}{\partial x} = 0. \quad CC \end{array} \right. \quad (19)$$

In the above equations, the following relationships are established:

$$\left\{ \begin{array}{l} B_1 = 2(\frac{l_0}{l_2})^2 + \frac{8}{15}(\frac{l_1}{l_2}) + 1, B_2 = \frac{L}{h}, B_3 = 5(\frac{l_0}{l_2})^2 + 2(\frac{l_1}{l_2}) \\ \mu_s = \frac{12\mu}{E(h/l_2)^2}, \quad \alpha = \frac{L_2}{L}, \quad \beta = \frac{b_1}{b_2} \quad (20) \\ \lambda^2 = \frac{24\epsilon_0 L V^2}{E h^3 g_0^3}, \quad \gamma = \frac{g_0}{b} \\ x_l = \begin{cases} 1-\alpha & CF \\ \frac{1-\alpha}{2} & CC \end{cases}, \quad x_u = \begin{cases} 1 & CF \\ \frac{1+\alpha}{2} & CC \end{cases} \end{array} \right.$$

3 SOLVING METHOD

Due to the nonlinearity of the governing equations, solving it is complicated and time-consuming. For this reason, in this research, differential quadrature method is used to solve these equations. According to this method, dimensionless displacements, as well as displacement derivatives at any arbitrary point are [22-23]:

$$\bar{w} = \sum_{j=1}^N l_j \bar{w}(\bar{x}_j) \quad (21)$$

$$\left. \frac{d^k}{d^k \bar{x}} \right|_{x_i} = \sum_{j=1}^N c_{ij}^{(k)} w(\bar{x}_j) \quad (22)$$

In the above equations, $c_{ij}^{(k)}$ is the weight functions and N denotes the number of nodes that are irregularly distributed over the entire domain (the length of the microbeam), and the position of each node subjected to the beginning of the beam is expressed as:

$$\bar{x}_i = \frac{1}{2} \left[1 - \cos \frac{\pi(i-1)}{N-1} \right] \quad (23)$$

Many methods have been proposed to calculate the weight functions in DQ, but one of the most accurate and easiest methods for determining the values of the weight functions and approximate the value of a function and its derivatives is given by Shu. Based on this method, the weight function for the derivative of $c_{ij}^{(1)}$ can be computed from the following formula:

$$\begin{aligned} c_{ij}^{(1)} &= \frac{\bar{L}(\bar{x}_i)}{(\bar{x}_i - \bar{x}_j)}, \quad i, j = 1, 2, \dots, N; i \neq j \\ c_{ii}^{(1)} &= \sum_{j=1, j \neq i}^N -c_{ij}^{(1)}, \quad i = 1, 2, \dots, N \\ \bar{L}(\bar{x}_i) &= \prod_{j=1}^N (\bar{x}_i - \bar{x}_j), \quad i, j = 1, 2, \dots, N; i \neq j \end{aligned} \quad (24)$$

To calculate the values of the weight functions in higher order derivatives can be used as follows:

$$\begin{aligned} c_{ij}^{(m)} &= m \left[c_{ij}^{(1)} c_{ii}^{(m-1)} \frac{c_{ij}^{(m-1)}}{(\bar{x}_i - \bar{x}_j)} \right], \quad i, j = 1, 2, \dots, N \\ c_{ii}^{(m)} &= \sum_{j=1, j \neq i}^N -c_{ij}^{(m)}, \quad i = 1, 2, \dots, N; m = 2, 3, \dots, N-1 \end{aligned} \quad (25)$$

By applying the DQ method to the governing equations (17), these are rewritten as follows:

$$\begin{cases} \beta(1+B_1\mu_s) \sum_{j=1}^N c_{ij}^{(4)} \bar{w}_{1j} - \beta B_3 \left(\frac{\mu_s}{30B_2} \right) \sum_{j=1}^N c_{ij}^{(6)} \bar{w}_{1j} = 0, & 0 \leq x \leq x_l, & CF, CC \\ (1-B_1\mu_s) \sum_{j=1}^N c_{ij}^{(4)} \bar{w}_{2j} - B_3 \left(\frac{\mu_s}{30B_2} \right) \sum_{j=1}^N c_{ij}^{(6)} \bar{w}_{2j} = \bar{Q}_i, & x_l \leq x \leq x_u, & CF, CC \\ \beta(1+B_1\mu_s) \sum_{j=1}^N c_{ij}^{(4)} \bar{w}_{3j} - \beta B_3 \left(\frac{\mu_s}{30B_2} \right) \sum_{j=1}^N c_{ij}^{(6)} \bar{w}_{3j} = 0, & x_u \leq x \leq 1, & CC \end{cases} \quad (26)$$

In the above equations, \bar{Q}_i is the distribution of force along the length of the microbeam as follows:

$$\bar{Q}_i = \frac{\lambda^2}{(1-\bar{w}_{2i})^2} + \frac{\gamma\lambda^2}{(1-\bar{w}_{2i})} \quad (27)$$

The governing equations and boundary conditions together form a system of nonlinear equations, which can be solved by solving methods such as Newton-Ruffson. However, here for solving this system, the equations are first linearized using the Taylor series of the applied force vector. Using a repetitive process below, the pull in voltages and displacement are obtained:

1- Using the Taylor Series Linear section, the initial force vector is rewritten as following form:

$$\bar{Q}_i = (2\lambda^2 + \gamma\lambda^2) \bar{w}_{2i} + \lambda^2 + \gamma\lambda^2 \quad (28)$$

Now, assuming the initial value of V_0 and solving equation (26) and boundary conditions, the displacement vector value \bar{w}_2 is obtained.

2- Equivalent to $\bar{w}_2^* = \bar{w}_2$ and placement \bar{w}_2^* in equation (27), a new force vector is obtained. Using the vector of force and rewriting the governing equations, we will have a matrix form:

$$K\bar{w}_2 = \bar{Q} \quad (29)$$

In the above equation, K represents a stiffness matrix. After solving the matrix equation, a new vector of \bar{w}_2^1 is obtained.

3- By replacing \bar{w}_2^1 instead of \bar{w}_2^* and repeating the second step, the displacement vector \bar{w}_2^2 will be obtained.

4- Repetition of the above step to the convergence of the deformation continues using the following tolerance:

$$Error = \sqrt{\frac{\sum (\Delta \bar{w}_2^m)^2}{\sum (\bar{w}_2^{m+1})^2}} \quad (30)$$

Where, $\Delta \bar{w}_2^m = \bar{w}_2^{m+1} - \bar{w}_2^m$ in the equation. The initial voltage increases until the stiffness matrix is singular or equation (29) is not satisfied. The last voltage that satisfies the deformation rate of equation (30) is the pull in voltage V_{PI} .

The above steps for \bar{w}_1 and \bar{w}_3 are also repeated and then summed together until the final pull in voltage and displacement are obtained.

4 RESULTS AND VERIFICATIONS

First, to ensure that the results are correct, the results of the current solution must be validated. Due to the fact that no laboratory and experimental work has been done on conductive polymer microbeams, the current solution method has been validated using the results in reference [4]. The mechanical properties and dimensions of the CF and CC are listed in “Table 1 and 2” respectively:

Table 1 Mechanical properties and dimensions of CF beam

$b_1 = 68\mu m$	$b_2 = 164\mu m$	$L = 140\mu m$
$L_2 = 94\mu m$	$h = 7\mu m$	$g_0 = 2\mu m$
$E = 78.5Gpa$	$\nu = 0.22$	$\rho = 19600kgm^{-3}$

But before verification, we need to make sure that the results of DQ are independent of the number of nodes which considered on the domain (length of the microbeam).

Table 2 Mechanical properties and dimensions of CC beam

$b_1 = 60\mu m$	$b_2 = 120\mu m$	$L = 500\mu m$
$L_2 = 100\mu m$	$h = 2\mu m$	$g_0 = 2\mu m$
$E = 78.5Gpa$	$\nu = 0.22$	$\rho = 19600kgm^{-3}$

“Fig. 3” shows the dependence of the pull in voltage on the number of nodes considered in DQ method for each of the different boundary conditions of the microbeam. As shown in “Fig. 3”, the pull in voltage after 10 nodes for CF beam becomes independent of the number of nodes.

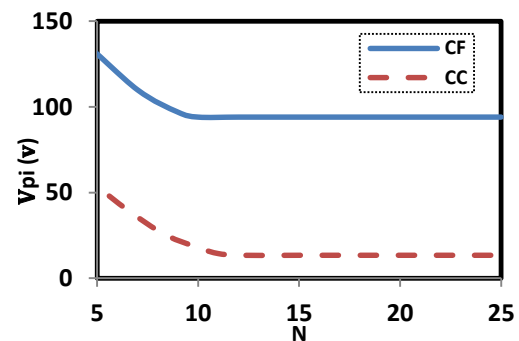


Fig. 3 Pull in voltage variation relative to the number of nodes considered in the DQ method.

Table 3 Comparison of the model results presented in reference [4] and the present solving method

Model type	CF Micro beam			CC Micro beam		
	[4]	Present work	Discrepancy Percent	[4]	Present work	Discrepancy Percent
Pull in voltage(v)	92.5	94.1	1.72	12.02	12.4	3.16

Table 4 Physical Properties of Conductive Polymers

Material	Conductivity (S/cm)	E (Gpa)	G (GPa)	$\rho(kg / m^3)$	ν
PANI	50	1.3	0.49	5210	0.32
PTs	1000	2.5	0.95	2230	0.32

In “Table 3”, the results of the current solution and the reference results [4] are compared. In reference [4], the couple stress theory is used, and the percentage of error obtained from the strain gradient theory and couple stress theory is also given in the table below, which according to reference [4], $l = 0$ is considered.

In the review of microbeams, $l_0 = l_1 = l_2 = l$ can be considered for reducing the parameters of the size effect and the convenience of discussing the results. With this assumption, the three size effects parameters are reduced to one parameter. In addition, this assumption helps to explain size effect parameter through simple diagrams without the reader being confused with multiple parameters. Moreover, this assumption makes it easier

to compare experimental results with the results of the strain gradient theory. On the other hand, determining a constant l through laboratory methods is easier than measuring three constants of l_0, l_1, l_2 .

For accuracy and reliability, the results of the dimensionless pull in voltage diagram and the dimensionless length ratio in “Figs. 4 and 5” are plotted for CF and CC stepped microbeam, respectively for value of $\beta = 0.2$ and compared with reference [4]. From the comparison of the results, it can be seen that the present solution is very well suited to the results of reference [4] that they used Finite element method. It is also seen that as the value of α increases, then the pull in voltage is decreased and then increased.

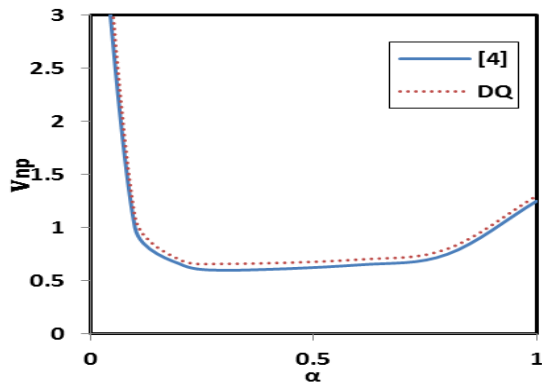


Fig. 4 Comparison of the results presented in reference [4] and the present work for CF beam.

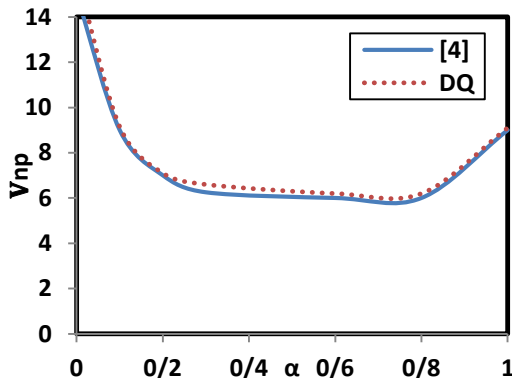


Fig. 5 Comparison of the results presented in reference [4] and the present work for CC beam.

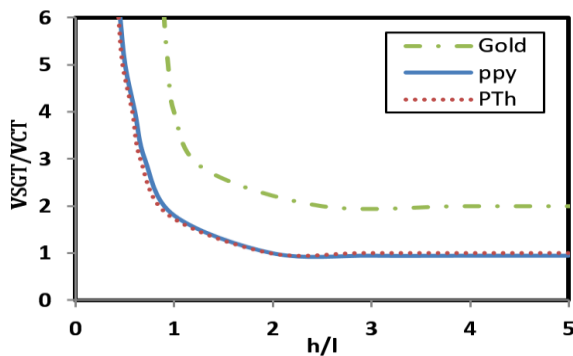


Fig. 6 The variation of the pull in voltage ratio versus the h/l for three materials.

4.1. Conductive Polymer

Work on the conductive polymers has grown over the last four decades. With the recent advances in micro/nano science and technology, the attention of many researchers have attracted the construction of conductive polymers in micro/nano dimensions. Polyaniline (PANI) and polythiophen (PTs) are among the polymers with the lowest and most conductivity. The

physical characteristics of these micro beams are given in “Table 4”.

In “Fig. 6”, the variations of the pull in voltage versus the ratio h/l of the two types of conductive polymer and also the gold material are plotted for CF microbeam, it is seen that by increasing the thickness ratio to the length parameter h/l , the pull in voltage ratio calculated by the theory of strain gradient theory V_{SGT} is reduced to the calculated voltage with the classical theory of V_{CT} . Although for the small values of h/l , the difference between the two theories becomes more significant. The physical properties of gold used in “Fig. 6” are:

$$\begin{cases} E = 98.5Gpa, & \rho = 19300kgm^{-3} \\ G = 27Gpa, & \nu = 0.44 \end{cases}$$

4.2. Effect of Length Scale Parameter

The variations of the pull in voltage versus the size effect of microbeam are shown in “Fig. 7”.

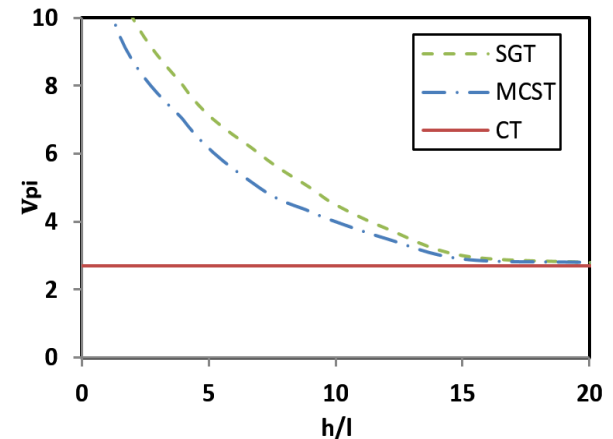


Fig. 7 Pull in voltage of microcantilever versus the h/l for different theories.

It can be seen that horizontal line is occurred when there is no size effect and the classical theory is used, in this case the pull in voltage is not a function of the size effect. However, in the strain gradient theory and modified couple stress theory, the pull in voltage is quite a function of the size effect, and also with the narrowing of the beam, this effect is more dependent on the length scale parameter. The close results of two non-classical theories in the graphs are clearly observed. It is worth mentioning that for $h/l < 5$, the difference between the classical and the non – classical theories for narrower beams is visible. In addition, strain gradient theory and modified couple stress theory are close to each other for $h/l > 5$, therefore it is importance to apply non-classical theories for the micro / nano scale dimensions.

4.3. Comparison of Theoretical Results with Experimental Results

Here, to obtain the length scale parameter of the conductive polymer (PANI) and compare with the article published by (Zhang and Chu 2007), microbeam without a step was considered. Using the strain gradient theory, for the conductive polymer (PANI) microcantilevers was considered with the geometrical properties as shown in “Table 1”. The pull-in voltages given by classical theory and the strain gradient theory

for microbeam with specifications given in “Table 1” are compared in “Table 5”. As it may be observed from “Table 5”, prediction of the pull in voltage from the classical theory are less than that of the experiment results. In other words, the classical theory predicts a lower stiffness for the beam with respect to the experimental results. Furthermore, the values of pull in voltage from the strain gradient theory are more than that of the values from the classical theory. Hence, it is deduced that the strain gradient theory may reduce the gap between the experiments and analytical simulations.

Table 5 Comparison between pull-in voltage predicted by classical and strain gradient theories with the experimental results given by Zhang et al [24] for beams with specifications given in “Table 1”

Cantilever Length (μm)	Pull-in Voltage based on the Classical Theory(V)	Pull-in Voltage based on the Strain gradient Theory(V)					Pull-in Voltage based on the experimental [24] (V)
		h/l=4	h/l=6	h/l=8	h/l=10	h/l=8.23(Optimum value)	
20	121.4	124.9	124.2	123.8	123.5	124.1	123.9
60	91.6	94.1	93.3	92.8	92.2	92.7	92.6
100	84.8	87.3	86.9	86.2	85.8	85.9	86.1
140	80.7	83.8	83.1	82.5	82.1	82.3	82.4

From the results of “Table 5”, it is concluded that the classical theory predicts the pull-in voltage less than the experiments. In other words, the classical theory predicts a lower stiffness for the beam with respect to the experimental results.

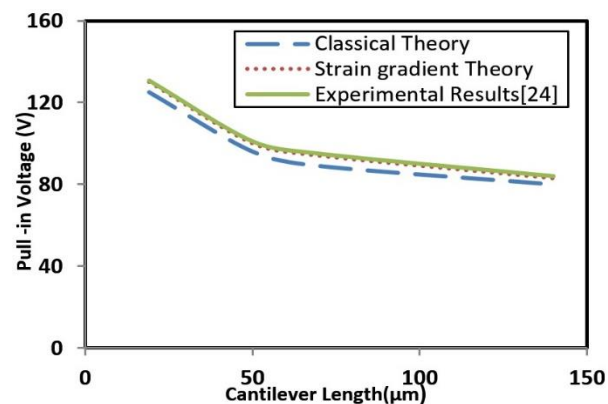


Fig. 8 Comparing the theoretical and experimental pull-in voltages for PANI.

On the other hand, the Strain gradient theory predicts more values for the pull-in voltage with respect to the classical theory. Hence, it is deduced that the Strain gradient theory may reduce the gap between the experiments and analytical simulations.

According to the least square error method, the best fit for the predictions of the strain gradient theory with the experimental results for various values of the beam length is achieved with $h/l = 8.23$. The pull-in voltages evaluated by the strain gradient theory with $h/l = 8.23$ are also presented in “Table 5”.

However, based on the trend of the predictions of the strain gradient theory, as discussed before, this theory can decrease the deviation of the classical theory predictions with the experimental results. With $h/l = 8.23$, the best fit for the strain gradient theory and the experimental results is achieved for the considered beams. Since the thickness of the beam is $h = 7\mu\text{m}$ (see “Table 1”), the length scale parameter is calculated as $l = 0.85\mu\text{m}$ (“Fig. 8”).

5 CONCLUSION

In the present paper, size dependent behavior was investigated for conductive polymer stepped microbeam with electrostatic force. The governing equations for the static deformation of the microbeam were obtained for two boundary conditions using the strain gradient theory and numerical solution of DQ. As the results show, the use of classical theory leads to incorrect results in microstructures, which have a longitudinal scale

parameter in comparison to their thickness, and non-classical theories such as strain gradient should be used. In addition, the results showed that the effect of size-dependent behavior is significantly increased by decreasing the thickness ratio to the length parameter of the microbeam. The results obtained in the design and modeling of microstructures are useful. In addition, the expensive and unavailable material can be replaced by conductive polymers as a new material.

REFERENCES

- [1] Rahnama, Mashhadi, A. N., and Moghimi Zand., M. M., Nonlinear Dynamics of Flexible Nanopositioning Systems with Geometrical Imperfection, *Microsystem Technologies*, Vol. 25, 2019, pp.1-11.
- [2] Noghrehabadi, A., Haghparast, A., Dynamic and Static Pull-In Instability of Partially Affected Nano-Cantilevers Using Modified Couple Stress Theory, *Modares Mechanical Engineering*, Vol. 16, 2016, pp. 81-91 (In Persian).
- [3] Sadeghi, M., Fathalilou, M., and Rezazadeh, G., Study on the Size Dependent Behavior of a Micro-Beam Subjected to a Nonlinear Electrostatic Pressure, *Modares Mechanical Engineering*, Vol.14, 2015, pp. 137-144 (In Persian).
- [4] Zhu, J., Yao, K., Dong, X., Huang, Q., and Liu, R., Pull-in Behavior of Electrostatically Actuated Stepped Microbeams, *International Journal of Modern Physics B*, Vol. 32, 2018, pp. 80-91.
- [5] Habibnejad Korayem, M., Habibnejad Korayem, A., Modeling of AFM with a Piezoelectric Layer Based on the Modified Couple Stress Theory with Geometric Discontinuities, *Applied Mathematical Modelling*, Vol. 45, 2017, pp. 439-456.
- [6] Rahaeifard, M., Ahmadian, M. T., On Pull-in Instabilities of Microcantilevers, *International Journal of Engineering Science*, Vol.87, 2015, pp. 23-31.
- [7] Rahaeifard, M., Kahrobaiyan, M. H., and Asghari, M., Static Pull-In Analysis of Microcantilevers Based on The Modified Couple Stress Theory, *Sensors and Actuators A*, Vol. 171, 2011, pp. 370-374.
- [8] Zhu, J., Liu, R., Sensitivity Analysis of Pull-in Voltage for Rf Mems Switch Based Modified Couple Stress Theory, *Applied Mathematics and Mechanics*, Vol. 74, 2015, pp.1-14.
- [9] Sedighi, H., Koochi, A., and Abadyan, M, Modeling the Size Dependent Static and Dynamic Pull – In Instability of Cantilever Nanoactuator Based on Strain Gradient Theory, *International Journal of Applied Mechanics*, Vol. 6, 2014, pp. 1-21.
- [10] Wang, X., Duan, G., Discrete Singular Convolution Element Method for Static, Buckling and Free Vibration Analysis of Beam Structures, *Applied Mathematics and Computation*, Vol. 234, 2014, pp. 36- 51.
- [11] Fathalilou, M., Rezaee, M., A Comparison Between Approaches for Solving Governing Nonlinear Equation of Vibration of Electrostatic Micro-Sensor, *Modares Mechanical Engineering*, No. 16, 2016, pp. 101-107 (In Persian).
- [12] Kumar, D., Sharma, R. C., Advances in Conductive Polymers, *Eur Polymer Journal*, Vol. 34, 1998, pp. 1053-1060.
- [13] Valentova, H., Stejskal, J., Mechanical Properties of Polyaniline, *Synthetic Metals*, Vol. 160, 2010, pp. 832-834.
- [14] Lang, U., Naujoks, N., and Dual, J., Mechanical Characterization of Pedot: Pss Thin Films, *Synthetic Metals*, Vol. 159, 2009, pp. 473- 479.
- [15] Cho, M., Cho, Y., Choi, H., and Jhon, M., Synthesis and Electrorheological Characteristics of Polyaniline-Coated Poly (Methyl Methacrylate) Microsphere: size effect, *Langmuir*, Vol. 19, 2003, pp. 5875- 5881.
- [16] Zhang, G., Chu, V., Electrostatically Actuated Conducting Polymer Microbridges, *Journal of applied physics*, Vol. 101, 2007, pp. 1-8.
- [17] Kumar, R., Singh, S., and Yadav, B., Conducting polymer: Synthesis, Properties and Applications, *International Advanced Research Journal in Science, Engineering and Technology*, Vol. 2, 2015, pp. 110- 124.
- [18] Lam, D. C. C., Yang, F., Chong A. C. M., Wang, J., and Tong, P., Experiments and Theory in Strain Gradient Elasticity, *Journal of the Mechanics and Physics of Solids*, Vol. 51, 2003, pp. 1477-1508.
- [19] Bostani, M., Mohammadi, A. K., Thermoelastic Damping in Microbeam Resonators Based on Modified Strain Gradient Elasticity and Generalized Thermoelasticity Theories, *Acta Mech*, Vol. 229, 2018, pp. 173-192.
- [20] Koochi, A., Sedighi, H., and Abadyan, M., Modeling the Size Dependent Pull- in Instability of Beam – Type Nems Using Strain Gradient Theory, *Latin American Journal of Solids and Structures*, Vol. 11, 2014, pp. 1806 -1829.
- [21] Fathalilou, M., Sadeghi, M., Rezazadeh, G., Nonlinear Behavior of Capacitive Micro – Beams Based on Strain Gradient Theory, *Journal of Mechanical Science and Technology*, Vol. 28, 2013, pp. 1141- 1151.
- [22] Shu, C., *Differential Quadrature and Its Application in Engineering*, London: Springer, 2000.
- [23] Shu, C., Du, H., A Generalized Approach for Implementing General Boundary Conditions in the Gdq Free Vibration Analysis of Plates, *International Journal of Solids and Structures*, Vol. 34, 1997, pp. 837-846.
- [24] Zhang, G., Chu, V., Electrostatically Actuated Conducting Polymer Microbridges, *Journal of Applied Physics*, Vol. 101, 2007, pp. 1-8.